# Correlated libration in liquid water

Cite as: J. Chem. Phys. 160, 114507 (2024); doi: 10.1063/5.0200094 Submitted: 24 January 2024 • Accepted: 4 March 2024 • Published Online: 21 March 2024







David P. Shelton<sup>a)</sup>



# **AFFILIATIONS**

Department of Physics and Astronomy, University of Nevada, Las Vegas, Nevada 89154-4002, USA

Note: This paper is part of the JCP Special Topic on Water: Molecular Origins of its Anomalies.

a) Author to whom correspondence should be addressed: shelton@physics.unlv.edu

#### **ABSTRACT**

The libration spectrum of liquid H<sub>2</sub>O is resolved into an octupolar twisting libration band at 485 cm<sup>-1</sup> and dipolar rocking-wagging libration bands at 707 and 743 cm<sup>-1</sup> using polarization analysis of the hyper-Raman scattering (HRS) spectrum. Dipole interactions and orientation correlation over distances less than 2 nm account for the 36 cm<sup>-1</sup> splitting of the longitudinal and transverse polarized bands of the dipolar rocking-wagging libration mode, while the intensity difference observed for the bands is the result of libration correlation over distances larger than 200 nm. The coupled rock and wag libration in water is similar to libration modes in ice. The libration relaxation time determined from the width of the spectrum is 36-54 fs. Polarization analysis of the HRS spectrum also shows long range correlation for molecular orientation and hindered translation, bending and stretching vibrations in water.

Published under an exclusive license by AIP Publishing. https://doi.org/10.1063/5.0200094

## I. INTRODUCTION

The many anomalous properties of liquid water are thought to be the result of the fluctuating disordered network of strong directional hydrogen bonds between the molecules. The most direct probe of the hydrogen bond network in water is the libration modes of the hydrogen bonded molecules, which have no counterpart in the single molecule spectrum. However, the libration spectrum observed by infrared absorption, Raman, and hyper-Raman scattering is broad and nearly featureless due to ultra-fast relaxation in liquid water.<sup>2-6</sup> Despite long study, the structure and extent of the hydrogen bonded network and the collective motions of the molecules are still unsettled questions.7

Hyper-Raman scattering (HRS) is the process where a Ramanshifted photon is emitted following excitation of the system by a pair of photons. Recently, the HRS spectra for H<sub>2</sub>O and D<sub>2</sub>O water and ice without polarization selection,<sup>5,6</sup> and H<sub>2</sub>O and D<sub>2</sub>O with polarization selection, 8,9 were measured to study the intermolecular vibrations. The dependence of HRS on the polarization of the incident and scattered light can be used to separate the contributions of TO (transverse optical) and LO (longitudinal optical) phonon modes for dipolar vibrations, and HRS has been used to investigate vibrational excitations in crystals, glasses, and liquids.<sup>10</sup> Recent HRS measurements with polarization selection have found transverse and longitudinal nonlocal vibration modes with correlation over distances comparable to the wavelength of the scattering wavevector for several glasses and molecular liquids. 9,11-14

The present work applies polarized HRS spectral measurement techniques and analysis, developed in previous studies of long range correlation in liquids, to the study of water.  $^{13-17}$  HRS is used to separate TO and LO contributions to the libration band, which are unresolved or unobserved by other spectroscopic techniques, and to assess the extent of nonlocal spatial correlation for the modes.

## II. HYPER-RAMAN SCATTERING

HRS is produced by oscillating molecular dipoles  $\mu = \beta E_{\omega}^2$ induced by the applied laser field  $E_{\omega}$ . The molecular response tensor  $\beta$  has odd parity and vanishes for centrosymmetric molecules. Vibrational modulation of  $\beta$  results in a dipole oscillation and scattered light frequency shifted from the laser second harmonic frequency. HRS from a liquid of uncorrelated randomly oriented molecules is the incoherent sum of the individual molecule HRS intensities, but HRS is sensitive to local and nonlocal molecular orientation correlations. 17,18

The polarization dependence of HRS carries information about the scattering system. Scattering configurations with incident and scattered light polarized either perpendicular or parallel to the horizontal scattering plane are denoted VV, HV, VH, and HH, where

V denotes vertical linear polarization, H denotes horizontal linear polarization, and the first and second letters refer to the incident and scattered light, respectively.

The third rank molecular first hyperpolarizability tensor  $\beta$ mediating HRS can be expressed in Cartesian tensor form or as the sum of irreducible spherical tensors.<sup>19</sup> The first rank irreducible spherical tensor contribution to  $\beta$  transforms as a vector and produces pure dipolar HRS for which  $I_{VV}/I_{HV}$  = 9, whereas the third rank irreducible spherical tensor contribution produces pure octupolar HRS for which  $I_{VV}/I_{HV} = 3/2$ . HRS due to the first rank irreducible spherical tensor (vector) contribution to  $\beta$  is sensitive to polar modes and correlations.

The vector  $\beta$  contributions for the molecules in a liquid form a homogeneous, isotropic, random vector field. The most general correlation tensor for such a field, in diagonal form, has transverse and longitudinal correlation functions as the diagonal components and produces HRS with components polarized longitudinal and transverse to the scattering wavevector. 17 Vector field correlations do not affect the octupolar  $\beta$  HRS contribution.

The HRS intensities for 90° scattering, including the vector and octupolar contributions, are given by

$$I_{VV} = (3/2)A_O + 9A_T, (1)$$

$$I_{HV} = A_O + A_T, (2)$$

$$I_{HH} = I_{VH} = A_O + (1/2)(A_T + A_L),$$
 (3)

where  $A_O$  is the octupolar contribution,  $A_T$  is the transverse dipolar contribution, and  $A_L$  is the longitudinal dipolar contribution. Polarized HRS data can be combined to determine  $A_O$ ,  $A_T$ , and  $A_L$  using the following relations:

$$A_O = (6/5)I_{HV} - (2/15)I_{VV},$$
 (4)

$$A_T = (2/15)I_{VV} - (1/5)I_{HV}, \tag{5}$$

$$A_L = (2/15)I_{VV} - (11/5)I_{HV} + I_{VH} + I_{HH}.$$
 (6)

The HRS intensities  $A_T$  and  $A_L$  are proportional to the diagonal components  $S_T(K)$  and  $S_L(K)$  of the spatial Fourier transform of the correlation tensor for vector  $\beta$ ,

$$S_{T}(K) = 4\pi \int_{0}^{\infty} \left\{ B_{T}(r) \left[ j_{0}(Kr) - \frac{j_{1}(Kr)}{Kr} \right] + B_{L}(r) \frac{j_{1}(Kr)}{Kr} \right\} g(r) r^{2} dr,$$
 (7)

$$S_{L}(K) = 4\pi \int_{0}^{\infty} \left\{ B_{L}(r) \left[ j_{0}(Kr) - \frac{2j_{1}(Kr)}{Kr} \right] + B_{T}(r) \frac{2j_{1}(Kr)}{Kr} \right\} g(r)r^{2} dr,$$
 (8)

where  $B_T(r)$  and  $B_L(r)$  are the diagonal components of the correlation tensor and  $j_n(x)$  are the spherical Bessel functions.<sup>17</sup> Correlation produces a sum of solenoidal and irrotational vector fields,

and the same expressions apply for  $\beta$  and transition  $\beta$  of correlated libration or vibration.

Transverse and longitudinal HRS intensities are equal in the case where intermolecular correlations are short range or absent,  $A_T = A_L$ . Unequal intensities for  $A_T$  and  $A_L$  requires correlation at distances comparable to or larger than the wavelength of the scattering wavevector. An explicit example is shown in Fig. 4 of Ref. 20 for the correlation function of a solenoidal vector field with  $r^{-3}$  asymptotic dependence, for which  $A_L = 0$ . HRS intensity ratio  $I_{HV}/I_{VH} \neq 1$  is an indicator for a dipolar mode with long range correlation, ranging from 2 for a pure transverse dipole mode to 0 for a pure longitudinal dipole mode. Vector field correlation with asymptotic  $r^{-3}$  dependence is required to produce such HRS polarization dependence.17

# III. EXPERIMENT

The experiment measures scattered light that is Raman-shifted from the laser second harmonic frequency. Linearly polarized pulses from a ps fiber laser and Nd:YAG (yttrium aluminum garnet) regenerative amplifier (output at  $\lambda = 1064$  nm with 25 kHz repetition rate, 26 ps pulse duration, 1 cm<sup>-1</sup> bandwidth) are focused to an 8  $\mu$ m diameter beam waist in the liquid sample in a standard square 10 mm fused silica fluorimeter cuvette. Scattered light at  $\theta = 90^{\circ}$  was collected and collimated using an aspheric lens (f = 4 mm), analyzed using a linear polarizer, focused into an optical fiber, and fiber-coupled to a scanning double grating monochromator and photon counting detector. The background count rate of the gated photomultiplier was 0.0016 s<sup>-1</sup>. The H<sub>2</sub>O sample (10 M $\Omega$  cm) flows in a loop containing the sample cell, conductivity cell, pump, ion exchange resin column, and 0.2 µm particle filter. The sample cell temperature was 25 °C for all measurements, and the average laser beam power in the water sample was 0.18 W. Absorption of laser light by the H<sub>2</sub>O sample increased the temperature at the focus to  $29^{\circ}$ C. Optical absorption in H<sub>2</sub>O is  $13 \times$ larger than in D<sub>2</sub>O, so high peak power ps pulses with lower average power were used to increase the HRS signal and reduce sample heating. The peak intensity was limited to 1 TW/cm<sup>2</sup> (<1/3 the intrinsic breakdown threshold) to prevent breakdown in nanobubbles at the focus and stimulated nonlinear effects,<sup>24</sup> and the resulting signal was 10× smaller than for D<sub>2</sub>O in a previous experiment.<sup>9</sup>

Spectra for polarization analysis were acquired from sequential 4000 cm<sup>-1</sup> scans with VV, HH, VH, and HV polarizations, repeated 284 times, and summed for each polarization configuration (4 × 1000 data points, total collection time 568 s for each data point). Spectra were acquired with numerical aperture NA = 0.375 and corrected for the effects of detector dead time, spectrometer spectral response, and the finite collection aperture. The spectrometer response has strong polarization dependence, so an effective depolarizer is required between the analyzing polarizer and the spectrometer. The combination of a long multimode fiber (40 m) followed by a liquid crystal polymer microarray depolarizer was used. The polarization and spectral response of the system was calibrated using a thermal light source and integrating sphere placed at the sample position. The spectrometer spectral slit width (SSW) was 20 cm<sup>-1</sup>. Further details of the polarization and spectral analysis, and the sample temperature calculation, are contained in the supplementary material of Ref. 9.

## IV. EXPERIMENTAL RESULTS

The HRS spectra for  $H_2O$  are shown in Figs. 1 and 2. The main spectral features are the reorientation mode at 0 cm $^{-1}$ , the hindered translation and libration modes below  $1000 \, \mathrm{cm}^{-1}$ , the bending mode at  $1646 \, \mathrm{cm}^{-1}$ , and the stretching mode at  $3423 \, \mathrm{cm}^{-1}$ .

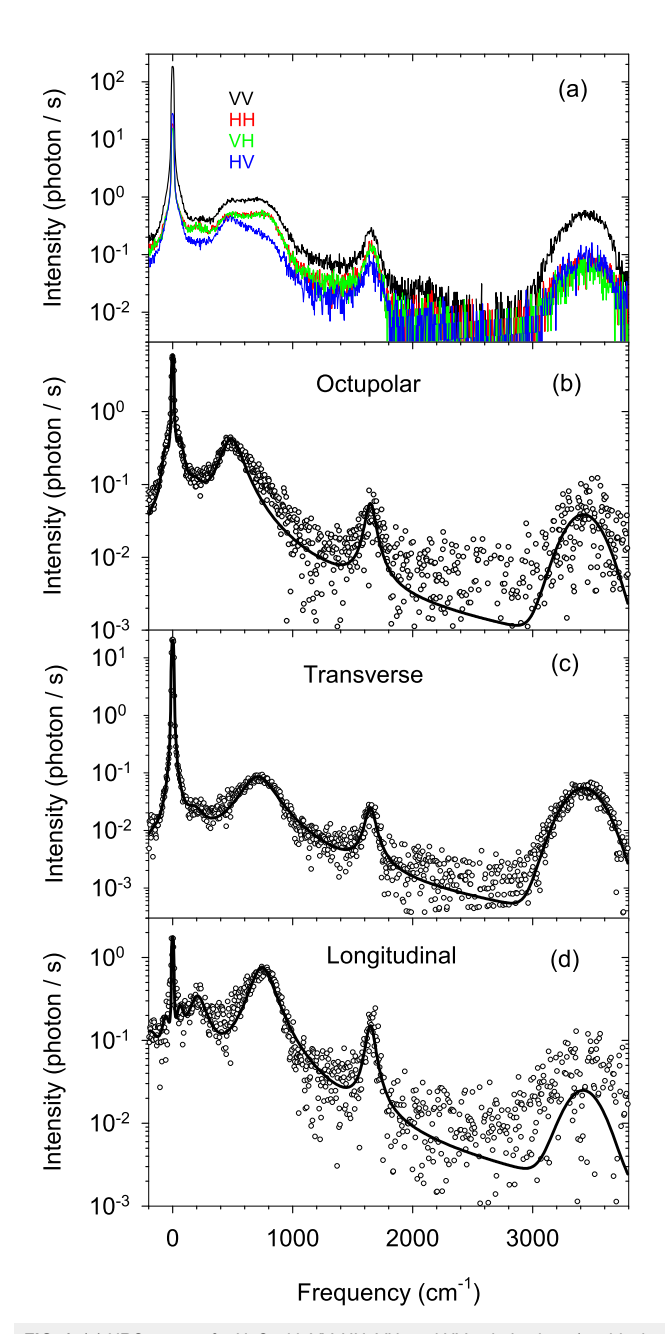


**FIG. 1.** (a) HRS spectra for  $H_2O$  with VV, HH, VH, and HV polarizations (top black, middle overlapping red and green, and bottom blue curves, respectively). The spectra in (a) are combined to find the (b) octupolar, (c) transverse dipolar, and (d) longitudinal dipolar HRS spectra. The curves show the fits to the O, T, and L spectra. Frequency  $\nu$  is the Stokes Raman shift.

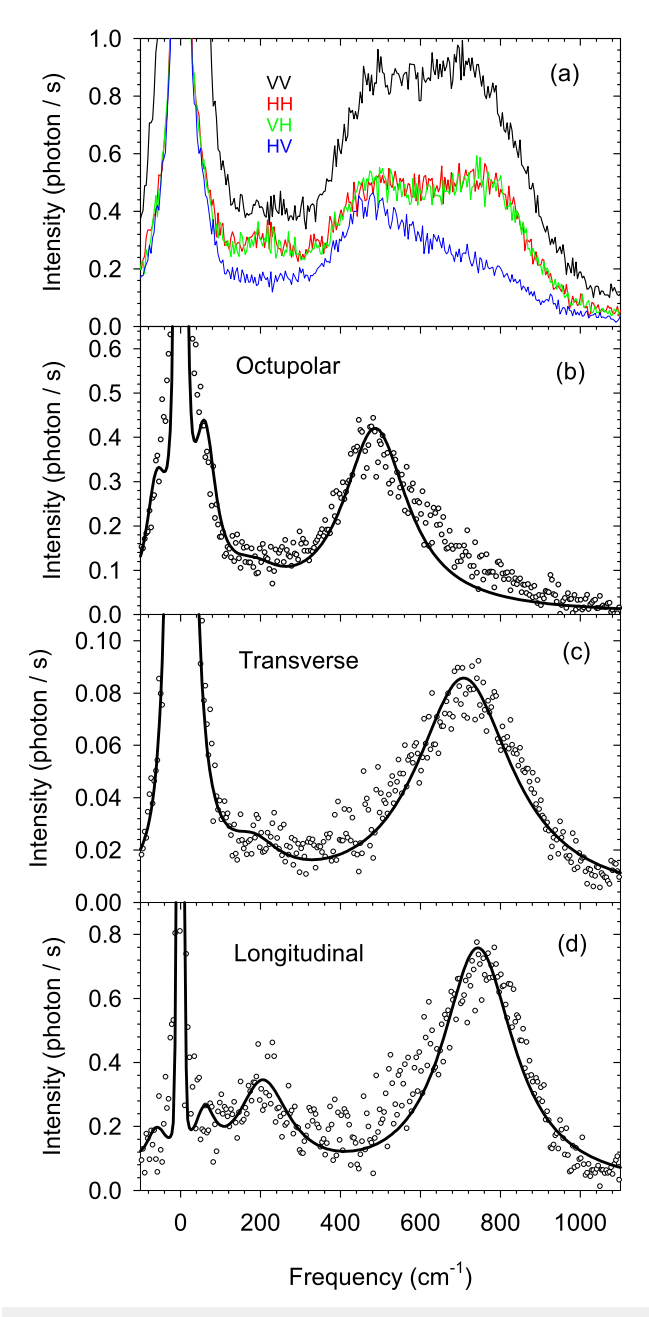


**FIG. 2.** Spectra from Fig. 1 with an expanded scale, over a 1200  ${\rm cm}^{-1}$  range including the libration band.

Figures 1(a) and 2(a) show the measured VV, HH, VH, and HV HRS intensities after background subtraction and correction for spectrometer spectral response. The VV, HH, VH, and HV polarized HRS data at each frequency are corrected for polarization mixing due to the finite collection aperture and combined to determine  $A_O$ ,  $A_T$ , and  $A_L$  at that frequency using Eqs. (4)–(6). The noise in the spectral data is increased using Eqs. (4)–(6), with the largest increase for  $A_L$ . Figures 1(b)–1(d) and 2(b)–2(d) show the resulting octupolar

(O), transverse dipolar (T), and longitudinal dipolar (L) spectra, and the functions fit to the data.

The  $A_O$ ,  $A_T$ , and  $A_L$  spectra are fit with a sum of Lorentzian functions,

$$I_i(\Delta \nu) = A_i / [1 + (\Delta \nu / \Delta \nu_i)^2], \tag{9}$$

except for the stretching mode, which was fit with a Gaussian function,

$$I_j(\Delta \nu) = A_j \exp\left[-(\Delta \nu/\Delta \nu_j)^2\right],\tag{10}$$

where  $\Delta v = (v - \bar{v}_j)$  is the detuning from resonance at Stokes frequency shift v for mode  $v_j$  with center frequency  $\bar{v}_j$  and width  $\Delta v_j$ . The calculated spectrum was multiplied by the factor

$$\left[1 + \exp\left(-hcv/kT\right)\right]^{-1} \tag{11}$$

to account for the Stokes/anti-Stokes asymmetry ( $kT/hc = 210 \text{ cm}^{-1}$  at 29 °C) and convolved with the spectrometer spectral slit function for the least squares fit to the experimental data.

Table I gives the parameters for the fitted curves in Figs. 1 and 2, and Table II gives mode intensity ratios determined from the data. Several constraints are imposed on the fit parameters for peaks outside the libration band. The central orientation mode is unresolved, so the 0.70 cm<sup>-1</sup> width for the orientation mode in the dipolar spectra is determined from the  $\tau = 7.60$  ps dielectric relaxation time at 29 °C using  $\Delta \nu (\text{cm}^{-1}) = (2\pi c\tau)^{-1}$ , <sup>25,26</sup> and the 2.80 cm<sup>-1</sup> width for the octupolar spectrum is set 4× larger in accordance with the jump model for reorientation in water. 27,28 This is similar to the results for D<sub>2</sub>O obtained from higher resolution spectra.<sup>9</sup> The position and width for the two hindered translation modes are set to the values observed by Raman scattering (except for the peak position for the second L translation mode).<sup>3,4</sup> For the bend and stretch modes, the position and width for the O and L peaks are set equal to the corresponding values obtained from the fit to the T peak. The intensities of the O and L bend (stretch) peaks are scaled to the intensity of the fitted T peak, using relative intensities  $A_O/A_T$  and  $A_L/A_T$ determined from the HRS signals integrated over the bend (stretch) band.

The libration band is decomposed into distinct but overlapping O, T, and L Lorentzian peaks. The fit is good except in the overlap region at about  $600~\rm cm^{-1}$ , where the uncertainty is largest. Inhomogeneous broadening can account for the skewness of the peaks but was not included in the present fit function. The long tails of the Lorentzian libration peaks account for the 2000 cm<sup>-1</sup> wide sloping background, which extends between the libration band and the stretching band in the HRS spectrum. Libration relaxation time  $\tau = (2\pi c \Delta v)^{-1} = 36$ , 49, or 54 fs is estimated assuming that the 147, 109, or 98 cm<sup>-1</sup> width of the Lorentzian libration peak is the result of lifetime broadening, with the fastest relaxation for the transverse libration mode. This is consistent with the sub-100 fs decay of librational excitation in H<sub>2</sub>O measured by a time resolved pump–probe experiment.<sup>29</sup>

Librational motion of a water molecule is composed of rocking (tilt of  $C_{2v}$  axis with the molecular plane fixed), wagging (tilt of  $C_{2v}$  axis and the molecular plane), and twisting (rotation around the  $C_{2v}$  axis) vibrations. Tilting the molecular axis modulates the molecular dipole vector and the vector component of  $\beta$ , so rocking and wagging librations are dipolar modes. Twisting does not

**TABLE I.** Parameters for the curves fit to the O, T, and L spectra in Figs. 1 and 2. The center frequency  $\bar{\nu}_j$  (cm<sup>-1</sup>), width  $\Delta \nu_j$  (cm<sup>-1</sup>), and intensity  $A_j$  (photon/s) are given for each mode, with the uncertainty in the last digit given in parentheses.

Mode	Symmetry	Center	Width	Intensity
Orientation	О	0	2.80	34 (1)
	T	0	0.70	784 (2)
	L	0	0.70	65 (10)
Translation 1	O	60	30	0.62(2)
	T	60	30	0
	L	60	30	0.29(3)
Translation 2	O	180	80	0.086(6)
	T	180	80	0.019(1)
	L	203(3)	80	0.42(1)
Libration	O	485(2)	98(2)	0.45(1)
	T	707(2)	147(3)	0.087(1)
	L	743(2)	109(2)	0.77(1)
Bend	O	1646	43	0.052
	T	1646(3)	43(4)	0.023(2)
	L	1646	43	0.14
Stretch	O	3423	211	0.038
	T	3423(3)	211(3)	0.053(1)
	L	3423	211	0.019

**TABLE II.** Relative O, T, and L intensities for modes of water, with the uncertainty in the last digit given in parentheses.

Mode	$A_O/A_T$	$A_L/A_T$
Orientation	0.044 (1)	0.08 (1)
Translation 1		
Translation 2	4.5 (4)	22 (2)
Libration	5.2 (1)	8.8 (2)
Bend	2.3 (2)	6.1 (4)
Stretch	0.72 (6)	0.36 (11)

modulate the dipole but does modulate the octupolar component of  $\beta$ . Therefore, the O mode at 485 cm<sup>-1</sup> is a twisting libration, while the dipolar T and L modes at 707 and 743 cm<sup>-1</sup> are rocking and/or wagging librations. The 36 cm<sup>-1</sup> L–T splitting of the dipolar libration modes observed for water is analogous to the LO–TO splitting of dipolar optical mode lattice vibrations in crystals.

A dipole mode with long range spatial correlation is indicated by intensities for HH and VH polarizations that are equal but different from the HV intensity, as seen in Figs. 1(a) and 2(a), and unequal transverse and longitudinal intensities  $A_T$  and  $A_L$ . This is the case for every mode shown in Figs. 1 and 2 and Tables I and II. The ratio  $A_L/A_T$  given in Table II shows that the orientation and stretching modes are dominantly transverse, while the translation, libration, and bending modes are dominantly longitudinal, similar to what was previously observed for  $D_2O$ .

# V. LIBRATION MODE L-T SPLITTING

Short range interactions, hydrogen bonds, and electrostatic interactions with the surrounding molecules produce the angular potential well for molecular libration. The orientation correlation of the dipolar molecules results in an average electric field in the mean direction of the molecular dipole, with dipole interaction energy  $U_D\cos\theta$  for a librating molecule. The harmonic oscillator frequency  $\omega^2 = k_\theta/I$  for small angular oscillations is changed by the added torque  $-k_{\theta D}\theta$  on the interacting dipoles, where  $k_{\theta D} = \theta^{-1} dU_D \cos\theta/d\theta$ . The libration frequency increment due to this dipole–dipole interaction is

$$\Delta\omega^2 = -U_D/I,\tag{12}$$

where I is the moment of inertia of the librating molecule. The dipole interaction energy per molecule for molecules with dipole moment  $\mu$  and number density  $\rho$  is

$$U_D = -\frac{\mu^2 \rho}{2\pi\epsilon_0} \int d^3r \, g_{12} \frac{3(\hat{\mu}_1 \cdot \hat{r}_{12})(\hat{\mu}_2 \cdot \hat{r}_{12}) - (\hat{\mu}_1 \cdot \hat{\mu}_2)}{r_{12}^3}, \quad (13)$$

where  $g_{12}$  is the pair distribution function,  $\hat{\mu}_1$  and  $\hat{\mu}_2$  are dipole unit vectors, and  $\hat{r}_{12}$  is the intermolecular unit vector. In terms of the correlation functions<sup>20</sup>

$$\langle (\hat{\mu}_1 \cdot \hat{r}_{12})(\hat{\mu}_2 \cdot \hat{r}_{12}) \rangle = B_L(r), \tag{14}$$

$$\langle \hat{\mu}_1 \cdot \hat{\mu}_2 \rangle = B_L(r) + 2B_T(r), \tag{15}$$

the interaction energy is

$$-U_D = (\mu^2 \rho/\epsilon_0) \int_0^\infty dr \ g(r) (B_L - B_T)/r. \tag{16}$$

The interaction energy is different for longitudinal and transverse correlated molecules. Combining Eqs. (12) and (16), one has

$$\Delta\omega_{LT}^2 = (2\pi c)^2 \Delta v_{LT}^2 = -U_D/I,$$
 (17)

where

$$v_L = (v_T^2 + \Delta v_{LT}^2)^{1/2}.$$
 (18)

The interaction energy  $U_D$  can be evaluated using the results from the molecular dynamics (MD) simulation using the TIP4P/2005 water model in Ref. 20. From the MD simulation, one has  $\mu=2.31$  D =  $7.7\times10^{-30}$  C m,  $\rho=3.34\times10^{28}$  m<sup>-3</sup>, and  $\mu^2\rho/\epsilon_0=2.23\times10^{-19}$  J. The integral in Eq. (16) is 0.1389 for  $B_L$  and -0.0170 for  $B_T$ , giving the interaction energy  $-U_D=3.48\times10^{-20}$  J. The integrals converge within 5% for r<1 nm and within 0.1% for r<3 nm. The interaction energy is dominated by short range interactions (r<3 nm) since the integrand in Eq. (16) decreases as  $r^{-6}$  at long range. Short range longitudinal correlation accounts for most of the L–T splitting.

For times short compared to the orientation relaxation time, the configuration of the hydrogen bond network is disordered and random but fixed, similar to ice. The libration band in the HRS spectrum of ice Ih consists of a narrow (31 cm<sup>-1</sup> FWHM) peak at 515 cm<sup>-1</sup> and a separate broad peak (212 cm<sup>-1</sup> FWHM) at

825 cm<sup>-1.5</sup> It is similar to the HRS libration band in the liquid but shifted up in frequency with a much more slowly relaxing twist mode. The broad high frequency component in both spectra may be assigned as dipolar rocking and wagging librations, which are strongly coupled and rapidly relaxing. Calculations for the proton-ordered phase of ice Ih (ice XI) find libration modes with coupled rocking or wagging on alternate neighbor molecules. <sup>30–33</sup> Such coupled rocking and wagging librations can be expected in liquid water.

The moments of inertia for H<sub>2</sub>O are  $I(10^{-47} \text{ kg m}^2) = 3.014$ , 1.930, and 1.004 for rock, twist, and wag.<sup>34</sup> An estimate for the effective moment of inertia for coupled rocking and wagging molecules is the average of the rocking and wagging moments. Evaluating Eq. (17) using  $I = 2.009 \times 10^{-47} \text{ kg m}^2$  for coupled rock and wag of H<sub>2</sub>O, one obtains  $\Delta \omega_{LT}^2 = 17.3 \times 10^{26} \text{ s}^{-2}$  and  $\Delta v_{LT}^2 = 4.88 \times 10^4 \text{ cm}^{-2}$ . Given the transverse libration mode frequency  $v_T = 707 \text{ cm}^{-1}$ , one calculates  $v_L = (v_T^2 + \Delta v_{LT}^2)^{1/2} = 741 \text{ cm}^{-1}$  for the longitudinal mode, as compared to  $v_L = 743 \text{ cm}^{-1}$  observed. The calculated L–T splitting is 34 cm<sup>-1</sup>, in good agreement with the observed splitting  $36 \pm 3 \text{ cm}^{-1}$  for the dipolar libration mode in H<sub>2</sub>O. This supports the assignment of this mode as a coupled rocking–wagging libration. A similar calculation for the 540 and 568 cm<sup>-1</sup> T and L dipole modes in D<sub>2</sub>O, where  $I(10^{-47} \text{ kg m}^2) = 5.777$ , 3.849, and 1.815 for rock, twist, and wag,<sup>35</sup> gives the calculated L–T splitting of 23 cm<sup>-1</sup> as compared to 28 cm<sup>-1</sup> observed.<sup>9</sup>

# VI. CORRELATED LIBRATION

The orientation pair correlation function for the permanent molecular dipoles at long range in a fluid of dipolar molecules is a solenoidal vector field with  $r^{-3}$  dependence. The interaction between the permanent molecular dipoles in the MD simulation for water in Ref. 20 produces a long range pair correlation with this form,  $B_L(r) = -2B_T(r) = (a/r)^3$  for r > 2 nm with a = 0.172 nm, where  $B_L$  and  $B_T$  are the orientation correlations longitudinal and transverse to the intermolecular vector. HRS, which is polarized transverse to the scattering wavevector K, is calculated for the orientation mode with this long range correlation using Eqs. (7) and (8).  $^{20}$ 

For the dipolar libration mode, the orientation correlation of the permanent molecular dipoles at short range accounts for the L–T splitting, but the intensity inequality with  $A_L/A_T=8.8$  also requires correlation of the libration transition dipoles over distances on the length scale of the wavelength of the scattering wavevector,  $r \ge \Lambda = 2\pi/K=284$  nm in this experiment. The observed longitudinal polarized HRS is produced by long range correlation of the transition dipoles with the asymptotic form for an irrotational vector field,  $B_L(r) = -2B_T(r) = -(b/r)^3$ , opposite to the correlation for the permanent dipoles.

The permanent dipole and vector  $\beta$  for  $H_2O$  are parallel to the molecular symmetry axis and both rotate with the molecule, so the direction of the oscillating transition dipole for a rocking or wagging libration is in a direction perpendicular to the mean direction of the permanent molecular dipole. If a pair of molecular dipoles point along the intermolecular direction, then the libration transition dipoles cannot. Therefore, increasing longitudinal correlation for dipole orientation decreases longitudinal correlation for the libration transition dipoles by the same amount.

Starting from zero correlation, this produces longitudinal correlations for the dipole and transition dipole with equal magnitude and opposite sign. The same argument applies for the transverse correlation.

A correlation function for a solenoidal vector field with the  $r^{-3}$  asymptotic dependence for dipole–dipole correlation is  $^{17}$ 

$$B_L(r) = [1 + (r/a)^2]^{-3/2},$$
 (19)

$$B_T(r) = [1 + (r/a)^2]^{-3/2} [1 - (3/2)r^2/(r^2 + a^2)].$$
 (20)

The Fourier transform of this correlation function using Eqs. (7) and (8) gives a transverse spectrum with  $S_T(0) = 2\pi a^3$  and  $S_L(0) = 0$ . This correlation function with  $a^3 = 5.072 \times 10^{-3}$  nm<sup>3</sup> is a good representation of the MD simulation results for H<sub>2</sub>O, except the short range structure for r < 2 nm.<sup>20</sup> A correlation function for an irrotational vector field with  $r^{-3}$  asymptotic dependence is<sup>17</sup>

$$B_T(r) = [1 + (r/b)^2]^{-3/2},$$
 (21)

$$B_L(r) = [1 + (r/b)^2]^{-3/2} [1 - 3r^2/(r^2 + b^2)].$$
 (22)

The Fourier transform of this correlation function gives a longitudinal spectrum with  $S_L(0) = 4\pi b^3$  and  $S_T(0) = 0$ . For  $2b^3 = a^3$ , these solenoidal and irrotational functions give long range correlation with the same magnitude but opposite sign.

The calculation of the longitudinal and transverse intensities for the libration spectrum of  $H_2O$  using Eqs. (7) and (8) is similar to the calculation for the orientation spectrum in Ref. 20. The correlation function is the sum of the delta function self-correlation at r=0 and the irrotational correlation function given by Eqs. (21) and (22) outside the excluded volume with radius  $r_1$ . The longitudinal and transverse intensities are

$$S_L(0) = 4\pi r_0^3 / 9 + 4\pi b^3 - (4\pi b^3 / 3) [1 + (b/r_1)^2]^{-3/2}, \tag{23}$$

$$S_T(0) = 4\pi r_0^3 / 9 + 0 - (4\pi b^3 / 3) [1 + (b/r_1)^2]^{-3/2}.$$
 (24)

The self-correlation contribution is  $4\pi r_0^3/9$ , where  $4\pi r_0^3/3 = \rho^{-1}$ ,  $\rho$  is the molecular density,  $r_0 = 0.1928$  nm, and  $r_1 \approx r_0$ . The contribution from the correlation functions Eqs. (21) and (22) inside the excluded volume has been subtracted from the integrals over all r. A more accurate calculation would use libration correlation functions obtained from a MD simulation instead of Eqs. (21) and (22) for r < 2 nm.

The observed ratio  $S_L/S_T = 8.8$  is obtained from Eqs. (23) and (24) for  $2b^3 = 5.16 \times 10^{-3}$  nm<sup>3</sup>, which is nearly equal to  $a^3 = 5.072 \times 10^{-3}$  nm<sup>3</sup> for the orientation correlation obtained from the MD simulation.<sup>20</sup> This indicates that the long range correlation function for the libration transition dipoles and libration transition vector  $\beta$  producing dominantly longitudinal librational HRS is equal and opposite to the long range orientation correlation function for the permanent molecular dipoles and is the result of

the long range orientation correlation of the permanent molecular dipoles.

#### VII. CORRELATED VIBRATION

The ratio  $A_L/A_T \neq 1$  seen in Table II for the bending and stretching modes indicates long range correlation for these molecular vibrations.

The bending vibration for an isolated  $H_2O$  molecule preserves the  $C_{2v}$  molecular symmetry, so the vector component of the transition  $\beta$  for the bending mode is parallel to the molecular dipole. If this is also the case in liquid water, then transition  $\beta$  for the bending mode will inherit the long range orientation correlation of the permanent dipole, and T polarized HRS should be observed for the bending mode. However, the HRS bending mode seen at 1646 cm<sup>-1</sup> is strongly L polarized.

The HRS stretching mode seen at 3423 cm<sup>-1</sup> is a composite band with several contributions. The oscillating dipole for the symmetric stretching vibration is oriented parallel to the permanent dipole of the molecule, so the oscillating dipoles for the symmetric stretching vibration will inherit the long range orientation correlation of the permanent molecular dipoles. This is also the case for the overtone of the bending vibration but not for the asymmetric stretching vibration. The T HRS polarization observed for the stretching band can be understood as a result of long range orientation correlation of the permanent dipoles, unlike the L HRS polarization observed for the bending mode.

## VIII. CONCLUSION

Polarized HRS analysis shows that the libration spectrum of water is composed of an octupolar twisting libration mode at 485 cm<sup>-1</sup> and a dipolar coupled rocking-wagging libration mode split into transverse and longitudinal polarized bands at 707 and 743 cm<sup>-1</sup>. Short range dipole orientation correlation (at distances less than 2 nm) accounts for the splitting of the dipolar rocking-wagging libration mode into longitudinal and transverse polarized bands. The coupled wag and rock libration in liquid water is similar to the calculated libration modes in ice. Each libration band is fit by a Lorentzian spectral function with width 98–147 cm<sup>-1</sup>, and the long tail of this Lorentzian accounts for the wide sloping background extending 2000 cm<sup>-1</sup> in the spectrum. The libration relaxation time determined from the Lorentzian width is 36-54 fs. Long range correlation of the librations (at distances greater than 200 nm) is required to account for the large intensity difference for the L and T spectra. Long range libration correlation revealed by the HRS analysis is the result of orientation correlation of the permanent molecular dipoles, and the resulting correlation is equal in magnitude but has opposite sign. Orientation correlation of permanent molecular dipoles can also account for the transverse polarization of the stretching vibration but not the observed longitudinal polarization for the bending vibration in liquid water.

# **ACKNOWLEDGMENTS**

This work was supported by the National Science Foundation (NSF) under Award No. CHE-1953941.

#### **AUTHOR DECLARATIONS**

## **Conflict of Interest**

The author has no conflicts to disclose.

## **Author Contributions**

**David P. Shelton**: Conceptualization (equal); Data curation (equal); Formal analysis (equal); Funding acquisition (equal); Investigation (equal); Methodology (equal); Validation (equal); Visualization (equal); Writing – original draft (equal); Writing – review & editing (equal).

# **DATA AVAILABILITY**

The data that support the findings of this study are available within the article.

#### REFERENCES

- <sup>1</sup>S. L. Bore and F. Paesani, "Realistic phase diagram of water from first principles data-driven quantum simulations," Nat. Commun. 14, 3349 (2023).
- <sup>2</sup>Y. Marechal, "The molecular structure of liquid water delivered by absorption spectroscopy in the whole IR region completed with thermodynamics data," J. Mol. Struct. **1004**, 146–155 (2011).
- <sup>3</sup>M. H. Brooker, G. Hancock, B. C. Rice, and J. Shapter, "Raman frequency and intensity studies of liquid H<sub>2</sub>O, H<sub>2</sub> <sup>18</sup>O and D<sub>2</sub>O," J. Raman Spectrosc. **20**, 683–694 (1989)
- <sup>4</sup>D. M. Carey and G. M. Korenowski, "Measurement of the Raman spectrum of liquid water," J. Chem. Phys. **108**, 2669–2675 (1998).
- <sup>5</sup>V. Korepanov, C.-C. Yu, and H. Hamaguchi, "Hyper-Raman investigation of intermolecular vibrations of water and ice," J. Raman Spectrosc. **49**, 1742–1746 (2018).
- <sup>6</sup>V. Korepanov, C.-C. Yu, and H. Hamaguchi, "Hyper-Raman spectral signatures of structured and de-structured hydrogen-bonded water," J. Raman Spectrosc. **53**, 1666–1668 (2022).
- <sup>7</sup>D. C. Elton and M. Fernandez-Serra, "The hydrogen-bond network of water supports propagating optical phonon-like modes," Nat. Commun. 7, 10193 (2016).
- <sup>8</sup>K. Inoue, Y. Litman, D. M. Wilkins, Y. Nagata, and M. Okuno, "Is unified understanding of vibrational coupling of water possible? Hyper-Raman measurement and machine learning spectra," J. Phys. Chem. Lett. 14, 3063–3068 (2023).
- <sup>9</sup>D. P. Shelton, "Hydrogen bond network modes in liquid water," Phys. Rev. B **108**, 174203 (2023).
- <sup>10</sup> V. N. Denisov, B. N. Mavrin, and V. B. Podobedov, "Hyper-Raman scattering by vibrational excitations in crystals, glasses and liquids," Phys. Rep. 151, 1–92 (1987).
- <sup>11</sup>B. Hehlen and G. Simon, "The vibrations of vitreous silica observed in hyper-Raman scattering," J. Raman Spectrosc. 43, 1941–1950 (2012).
- <sup>12</sup>V. Rodriguez, "New structural and vibrational opportunities combining hyper-Rayleigh/hyper-Raman and Raman scattering in isotropic materials," J. Raman Spectrosc. 43, 627–636 (2012).
- $^{1\bar{3}}$ D. P. Shelton, "Long-range correlation of intra-molecular and inter-molecular vibration in liquid CCl<sub>4</sub>," J. Chem. Phys. **154**, 034502 (2021).
- <sup>14</sup>D. P. Shelton, "Long range correlation of molecular orientation and vibration in liquid CDCl<sub>3</sub>," AIP Adv. **12**, 105008 (2022).

- <sup>15</sup>D. P. Shelton, "Accurate hyper-Rayleigh scattering polarization measurements," Rev. Sci. Instrum. **82**, 113103 (2011).
- <sup>16</sup>D. P. Shelton, "Long-range orientation correlation in water," J. Chem. Phys. 141, 224506 (2014).
- <sup>17</sup>D. P. Shelton, "Long-range correlation in dipolar liquids probed by hyper-Rayleigh scattering," J. Chem. Phys. **143**, 134503 (2015); Erratum **146**, 199901 (2017).
- <sup>18</sup>D. P. Shelton, "Polarization and angle dependence for hyper-Rayleigh scattering from local and nonlocal modes of isotropic fluids," J. Opt. Soc. Am. B 17, 2032–2036 (2000); Erratum 34, 1550 (2017).
- <sup>19</sup>P. D. Maker, "Spectral broadening of elastic second-harmonic light scattering in liquids," Phys. Rev. A 1, 923–951 (1970).
- <sup>20</sup>D. P. Shelton, "Structural correlation in water probed by hyper-Rayleigh scattering," J. Chem. Phys. **147**, 154501 (2017).
- <sup>21</sup>S. Kedenburg, M. Vieweg, T. Gissibl, and H. Giessen, "Linear refractive index and absorption measurements of nonlinear optical liquids in the visible and near-infrared spectral region," Opt. Mater. Express 2, 1588–1611 (2012).
- <sup>22</sup>J. P. Gordon, R. C. C. Leite, R. S. Moore, S. P. S. Porto, and J. R. Whinnery, "Long-transient effects in lasers with inserted liquid samples," J. Appl. Phys. 36, 3–8 (1965).
- <sup>23</sup> A. Linan and V. N. Kurdyumov, "Laminar free convection induced by a line heat source, and heat transfer from wires at small Grashof numbers," J. Fluid Mech. 362, 199–227 (1998).
- <sup>24</sup> V. A. Babenko, N. F. Bunkin, and A. A. Sychev, "Role of gas nanobubbles in non-linear hyper-Raman scattering of light in water," J. Opt. Soc. Am. B 37, 2805–2814 (2020).
- <sup>25</sup>B. Kutus, A. Shalit, P. Hamm, and J. Hunger, "Dielectric response of light, heavy and heavy-oxygen water: Isotope effects on the hydrogen-bonding network's collective relaxation dynamics," Phys. Chem. Chem. Phys. 23, 5467–5473 (2021).
- <sup>26</sup>R. Buchner, J. Barthel, and J. Stauber, "The dielectric relaxation of water between 0°C and 35°C," Chem. Phys. Lett. **306**, 57–63 (1999).
- <sup>27</sup>D. Laage and J. T. Hynes, "A molecular jump mechanism of water reorientation," Science 311, 832–835 (2006).
- <sup>28</sup> D. Laage and J. T. Hynes, "On the molecular mechanism of water reorientation," J. Phys. Chem. B 112, 14230–14242 (2008).
- <sup>29</sup>S. Ashihara, N. Huse, A. Espagne, E. T. J. Nibbering, and T. Elsaesser, "Ultrafast structural dynamics of water induced by dissipation of vibrational energy," J. Phys. Chem. A 111, 743–746 (2007).
- <sup>30</sup> K. Iwano, T. Yokoo, M. Oguro, and S. Ikeda, "Propagating librations in ice XI: Model analysis and coherent inelastic neutron scattering experiment," J. Phys. Soc. Jpn. 79, 063601 (2010).
- <sup>31</sup> K. Abe, T. Miasa, Y. Ohtake, K. Nakano, M. Nakajima, H. Yamamoto, and T. Shigenari, "Raman spectra of proton ordered XI phase ice crystal," J. Korean Phys. Soc. **46**, 300–302 (2005).
- <sup>32</sup>T. Shigenari and K. Abe, "Vibrational modes of hydrogens in the protonordered phase XI of ice: Raman spectrum above 400 cm<sup>-1</sup>," J. Chem. Phys. **136**, 174504 (2012).
- <sup>33</sup>P. Zhang, Z. Wang, Y.-B. Lu, and Z.-W. Ding, "The normal modes of lattice vibrations of ice XI," Sci. Rep. 6, 29273 (2016).
- <sup>34</sup>R. T. Hall and J. M. Dowling, "Pure rotational spectrum of water vapor," J. Chem. Phys. 47, 2454–2461 (1967).
- $^{\bf 35}R.$  A. Toth, "D $_2^{\bf 16}O$  and D $_2^{\bf 18}O$  transition frequencies and strengths in the  $\nu_2$  bands," J. Mol. Spectrosc. **162**, 41–54 (1993).
- <sup>36</sup>M. S. Wertheim, "Exact solution of the mean spherical model for fluids of hard spheres with permanent electric dipole moments," J. Chem. Phys. **55**, 4291–4298 (1971)
- $^{37}$ J.-P. Hansen and I. R. McDonald, *Theory of Simple Liquids*, 4th ed. (Academic Press, 2013).